Feasible Point Pursuit and Successive Convex Approximation for Transmit Power Minimization in SWIPT-Multigroup Multicasting Systems

Sumit Gautam, *Member IEEE*, Eva Lagunas, *Senior Member IEEE*, Symeon Chatzinotas, *Senior Member IEEE*, and Björn Ottersten, *Fellow IEEE.*

***Abstract*—We consider three wireless multi-group (MG) multicasting (MC) systems capable of handling heterogeneous user types viz., information decoding (ID) specific users with conventional receiver architectures, energy harvesting (EH) only users with non-linear EH module, and users with joint ID and EH capabilities having separate units for the two operations, respectively. Each user is categorized under unique group(s), which can be of MC type specifically meant for ID users, and/or an energy group consisting of EH explicit users. The joint ID and EH users are a part of both EH group and single MC group. We formulate an optimization problem to minimize the total transmit power with optimal precoder designs for the three aforementioned scenarios, under certain quality-of-service constraints. The problem may be adapted to the well-known semi-definite program and solved via relaxation of rank-1 constraint. However, this process leads to performance degradation in some cases, which increases with the rank of solution obtained from the relaxed problem. Hence, we develop a novel technique motivated by the feasible-point pursuit successive convex approximation method in order to address the rank-related issue. The benefits of proposed method are illustrated under various operating conditions and parameter values, with comparison between the three above-mentioned scenarios.**

***Index Terms*—Feasible point pursuit and successive convex approximation (FPP-SCA), multi-group (MG) multicast (MC) precoding, simultaneous wireless information and power transmission (SWIPT), transmit power optimization, semi-definite program (SDP).**

I. Introduction

The evolution of wireless communication technologies is now happening at an even faster pace in comparison to previous generations. In this process, several critical issues like the increasing performance and capacity needs, power management at the complex hardware set-ups, and demands for energy-efficient algorithms at the wireless devices, still remain great challenges to address. Following these insistent demands, another challenge is posed in the form of battery limitations at the wireless devices, wherein their high power consumption leads to frequent recharging. To address this, two possibilities arise; optimization of power consumption at the devices, or seeking alternative energy harvesting (EH) techniques for recharging [2]. The latter prospect invokes a renewed research interest leading towards investigation of systems which ensure coexistence of heterogeneous user devices, including information decoding (ID) only, specific to EH, and ones performing ID and EH concurrently [3], [4].

Several advantages of adopting Multiple-Input Single-Output (MISO) set-up can be seen from the perspective of ID users [5]. An interesting idea to perform joint radio-frequency (RF) information and energy transmission was proposed in [6], which was later incorporated to the multi-user MISO case in [2], [7]. Regarding the EH modules, separated architectures (SA) seem more promising in contrast to other proposed EH models due to reduced hardware complexities and no-extra optimization parameter(s) [8]. On the other hand, transmit precoding can enhance the channel capacity and diversity in multi-user MISO systems significantly [9]. Another potential technique in this direction is termed Multi-group (MG) Multicasting (MC), where its benefits with precoding are illustrated in [10]–[12]. However, MG-MC precoding problem for only a single group multicast was found to be NP-hard in [9]. With an assumption of a linear EH module, certain works have investigated joint transmission of information and energy in an MG-MC scenario [13], [14]. Noticeably, the above mentioned works neither takes into consideration the co-existence aspect of heterogeneous user types, nor the non-linear EH aspect at the intended users within the MG-MC framework.

In this work, we investigate three systems with the MG-MC framework, where the goal is to minimize the total transmit power via precoder designing mechanism, in order to serve heterogeneous types of users. The single transmitter is assumed to be equipped with multiple antennas that enable the precoders to meet the demands at the intended devices via beamforming technique. Herein, the formulated optimization problem (as mentioned above) is found to be non-convex. However, it can be converted into a semi-definite programming (SDP) problem and solved using known transformations and relaxations. Even though suitable solutions are typically obtained, this method reveals a lot of uncertainties revolving around the approximations. Therefore, we propose a novel technique as an alternative to solving the SDP, termed as Feasible Point Pursuit - Successive Convex Approximation for energy optimization (FPP-SCA-e), which is based on modified FPP-SCA [15]. The proposed technique yields significant gains both in terms of performance as well as the computa-

The authors are with the Interdisciplinary Centre for Security, Reliability and Trust (SnT), University of Luxembourg, L-2721 Luxembourg. E-mail: {sumit.gautam, eva.lagunas, symeon.chatzinotas, bjorn.ottersten}@uni.lu

Part of this work has been published in IEEE International Conference on Communications 2020 (ICC'20) [1].

The research leading to these results has received funding from the Luxembourg National Research Fund (FNR), Luxembourg, under the FNR-FNRS bilateral - InWIP-NET: Integrated Wireless Information and Power Networks (R-AGR-0700-10-X).

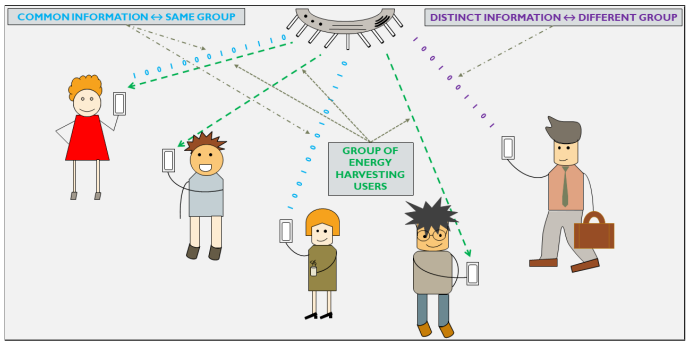

Fig. 1: Basic schematic of the considered framework.

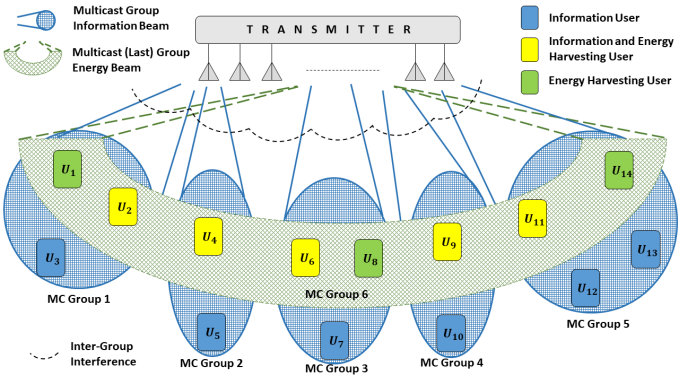

Fig. 2: Separate Multicast and Energy Precoding Design.

tional complexity. To summarize, the main contributions and novelty of this paper are highlighted below.

(a) We compare three novel MG-MC precoding frameworks which deals with co-existence of three user types capable of ID, EH, and joint ID and EH, respectively, by investigating the newly devised problem formulations. In this context, it is important to mention that most of the existing works in the literature do not consider co-existence of multiple user types for analysis.

(b) We provide adequate transformation to reduce the non-linear EH constraint to a linear form. Without loss of generality, this transformation is useful not only for the solution of the considered problem, but potentially even more challenging problems with similar constraints.

(c) To address the limitations of SDP and the rank-concerns related to the SDR-based solutions, we propose a novel technique called FPP-SCA-e, which does not only takes into consideration the EH constraint in contrast to the traditional FPP-SCA method [15], [16], but also provides significant gains over the SDR-based approximations while ensuring unit rank solutions for corresponding precoder metrics. The FPP-SCA technique is well known, however, it needs to be adapted according to the considered novel framework.

(d) We discuss the benefits of separate information and/or energy precoder design over other designs used for comparison, to motivate its practical implementation, while additionally drawing a comparative study between the proposed FPP-SCA-e and SDR techniques which has not been considered in the literature.

The remainder of this paper is organized as follows. Section II provides an introduction to the system model. The problem formulation and the proposed solution are presented in Section III. Numerical results are shown in Section IV, followed by concluding remarks in Section V.

Notation: In the remainder of this paper, bold face lower case and upper case characters denote column vectors and matrices, respectively. The operators $(\cdot)^{\dagger}$, $|\cdot|$ and $\otimes$ correspond to the conjugate transpose, the absolute value and the Kronecker product, respectively. An identity matrix of $Y \times Y$ dimensions is denoted as $\mathbf{I}_Y$, where its y^{th} column is represented as $\mathbf{e}_y$. Calligraphic indexed characters denote sets. $\mathbb{R}_{\kappa}^{+}$ denotes the set of real positive κ-dimensional vectors.

II. System Model

In this work, we assume that K users $(\mathcal{U}_1, \ldots, \mathcal{U}_K)$ are served via single transmit source equipped with M antennas. The heterogeneous receiver types, viz-a-viz., ID, EH, and joint ID and EH are categorized within $Z+1$ groups. In the case with both ID and EH operations, corresponding user adopts the separated architecture (SA) for SWIPT [8], with two separate RF antennas and chains for carrying out the desired operations.

As illustrated in Fig. 1, a precoder-based multi-antenna transmitter and a variety of users intending to carrying out the ID, EH, and joint ID and EH processes accordingly, compose the overall system. In this regard, the users demanding same information are categorized under a unique MC group, while the user(s) with different information demand are categorized under a different MC group. In simple terms, the user(s) demanding same set of information are categorized under one MC group, while there can be multiple MC groups present in the system. In order to meet the energy requirements, an additional group is composed of EH users. It is noteworthy that a user may be present in either of the MC groups and/or the EH group. To serve the heterogeneous users, different models of precoding may be adopted for investigation.

Herein, we examine three precoder design schemes for optimization of total transmit power, described as follows

(a) *Separate Multicast and Energy Precoding Design (SMEP)*: We aim at designing $(Z+1)$ precoders, where Z precoders are designated to serve Z MC groups and an additional precoder exclusively takes care of $(Z+1)^{\text{th}}$ group with EH users. (*Ref.* Fig. 2)

(b) *Joint Multicast and Energy Precoding Design (JMEP)*: We target the design of Z precoders for fulfilling the ID and EH demands of respective Z multicast precoders and the additional group with EH users. Specifically, there is no particular precoder for serving EH users. (*Ref.* Fig. 3)

(c) *Per-User Information and/or Energy Precoding Design (PIEP)*: Herein, design of K precoders (equal to the number of users) is intended, where each user is served by its dedicated precoder. (*Ref.* Fig. 4)

In the context of user categorizations within the groups, several methods may be adopted. Correspondingly, one such method with channel co-linearity and orthogonality based user grouping is considered in [17] where initially $(Z+1)$ users

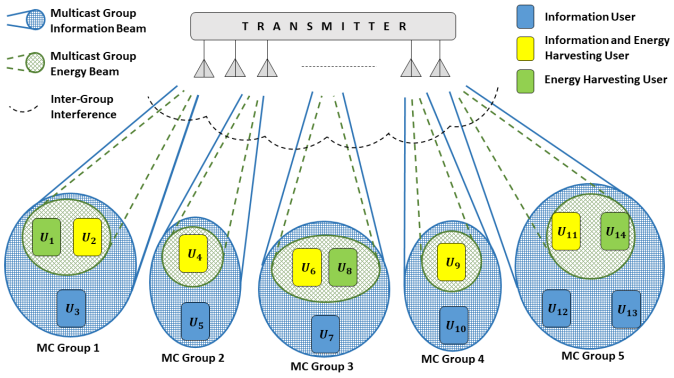

Fig. 3: Joint Multicast and Energy Precoding Design.

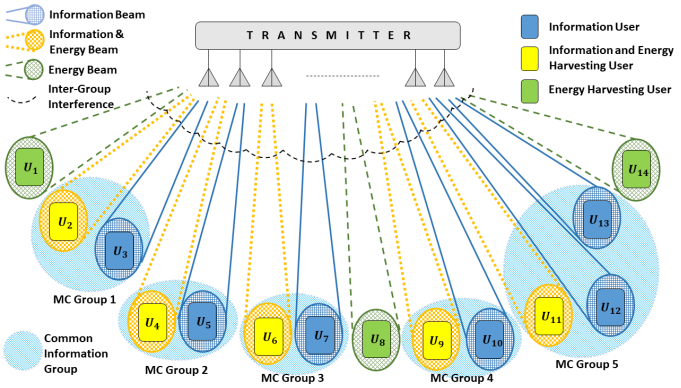

Fig. 4: Per-User Information and/or Energy Precoding Design.

(same as number of groups) with most orthogonal channels are considered as different groups. Further, the unallocated users are assigned to the groups based on co-linearity with the existing users in the groups. In [18], the authors consider message based user grouping where it is proved that ad-hoc user clustering is optimal for massive multiple input multiple output (MIMO) systems under max-min SINR design criterion. We assume Z MC groups and the $(Z+1)^{\text{th}}$ group with EH users, where all the classifications are already known. Such method is used for analytical convenience wherein we assume that all the users are already categorized among various groups and these arrangements are known a priori [13], [14]. In this regard, we define the following variable to assist the precoder design metrics for three scenarios interchangeably

$$\Psi = \begin{cases} Z+1 & : \quad \text{SMEP} \ \rightarrow \ \psi(a). \\ Z & : \quad \text{JMEP} \ \rightarrow \ \psi(b). \\ K & : \quad \text{PIEP} \ \rightarrow \ \psi(c). \end{cases} \tag{1}$$

Let $\mathcal{Z}_k$ denote the k^{th} multicast/energy group of users such that $\mathcal{Z}_k \cap \mathcal{Z}_\ell = \varnothing$, $\forall k, \ell = \{1, \ldots, \Psi\}$ and $k \neq \ell$; whereas in the case of EH, the user harvests energy using all the possible multicast signals[1].

Define $\mathbf{w}_k$ as the related $M \times 1$ complex precoder weight vector to serve the ID and/or EH user(s) corresponding to $\mathcal{Z}_k$. The transmitter emits the signal $\mathbf{x}(t) = \sum_{k=1}^{\Psi} \mathbf{w}_k s_k(t)$, where $s_k(t)$ is the corresponding information and/or energy signal. The signals for each group $\{s_k(t)\}_{k=1}^{\Psi}$ are mutually uncorrelated to each other with zero mean and unit variance. Distinct ID and EH signal waveform designing [19] motivates the use of SA-based SWIPT receiver architecture. The total transmit power is represented as $\sum_{k=1}^{\Psi} \mathbf{w}_k^\dagger \mathbf{w}_k$.

The signal received at the i^{th} user is given by $u_i(t) = \mathbf{h}_i^\dagger \mathbf{x}(t) + n_{R,i}(t)$, where $\mathbf{h}_i$ is the $M \times 1$ conjugated channel vector for the corresponding user and $n_{R,i}(t)$ is the additive zero mean Gaussian noise at the corresponding i^{th} user's receiving antenna equipment with a noise variance of $\sigma_{R,i}^2$. The source signals are uncorrelated with $n_{R,i}(t)$. The signal at the ID module of i^{th} receiver equipment is expressed as

$$u_{D,i}(t) = (\mathbf{h}_i^\dagger \mathbf{x}(t) + n_{R,i}(t)) + n_{D,i}(t), \tag{2}$$

where $n_{D,i}(t)$ is the additional zero-mean Gaussian noise with a variance of $\sigma_{D,i}^2$ which mainly arise due to the circuitry associated with the ID block of the i^{th} receiver.[2] The signal-to-interference-and-noise ratio (SINR) at the i^{th} receiver as a part of the k^{th} multicast group $\mathcal{Z}_k$, is given by

$$\Upsilon_i = \frac{|\mathbf{w}_k^\dagger \mathbf{h}_i|^2}{\sum_{\ell \neq k} |\mathbf{w}_\ell^\dagger \mathbf{h}_i|^2 + \sigma_{R,i}^2 + \sigma_{D,i}^2}, \forall \ell = \{1, \ldots, \Psi\}. \tag{3}$$

The signal utilized for EH operation at the i^{th} receiver is

$$u_{E,i}(t) = \mathbf{h}_i^\dagger \mathbf{x}(t) + n_{R,i}(t). \tag{4}$$

Therefore, the energy extracted by the EH unit of i^{th} receiver is given as, $\mathcal{E}_i^{\mathcal{L}} = \zeta_i (\sum_{k=1}^{\Psi} |\mathbf{w}_k^\dagger \mathbf{h}_i|^2 + \sigma_{R,i}^2)$, where $0 < \zeta_i \leq 1$ is the energy conversion efficiency of the EH unit at the corresponding receiver. Note that $\mathcal{E}_i^{\mathcal{L}}$ is theoretically valid in order to represent a linear EH operation, however its practical implementation is doubtful. Thus, this calls for the adoption of a non-linear EH model [20] at the i^{th} receiver, defined as

$$\mathcal{E}_i^{\mathcal{N}} = \frac{\mathcal{E}'}{1-\phi} \cdot \left(\frac{1}{1 + e^{(-\alpha(\sum_{k=1}^{\Psi} |\mathbf{w}_k^\dagger \mathbf{h}_i|^2) + \alpha\beta)}} - \phi \right), \tag{5}$$

where $\phi \triangleq \frac{1}{1+\exp(\alpha\beta)}$, the constant $\mathcal{E}'$ is obtained by determining the maximum harvested energy on the saturation of the energy harvesting circuit, and α and β are specific for the capacitor and diode turn-on voltage metrics at the EH circuit. Practically, a standard curve-fitting tool based on analytical data may be used to decide the appropriate values of $\mathcal{E}'$, α, and β. We assume normalized time slots to use the terms *power* and *energy* interchangeably.

Regarding the utilization of radio resources by the users, it is important to mention that the precoder designs are intended to take care of appropriately transferring the information to ID users and energy to EH users. This mechanism is realised by performing the optimization for precoder designs, so that the radio resource is managed via adequate beamforming. Additionally, the interference aspect is also managed by the precoders present at the transmitter. These aspect will be discussed later in detail.

In the succeeding section, we formulate an optimization problem corresponding to precoder designs for minimization

[1]The other MCs are primarily taken into consideration due to interference causing side-lobes other than the desired MC, which is beneficial for EH.

[2]It is noteworthy that the precoder is responsible for managing the radio resources for the intended users from the transmitter via multiple antennas.

of the total transmit power in the three aforementioned scenarios. Suitable solutions are obtained by employing adequate transformations and relaxations.

III. Transmit Power Minimization

In this section, we formulate the optimization problem to minimize the overall transmit power subjected to minimum SINR and minimum EH constraints at the corresponding users/groups.

A. Problem Formulation

The overall optimization problem (encapsulating the three considered scenarios) to ensure the co-existence of the heterogeneous user types in the MG-MC precoding scheme can subsequently be written in its analytical form as follows

$$(P1): \min_{\{\mathbf{w}_k\}_{k=1}^{\Psi}} \sum_{k=1}^{\Psi} \mathbf{w}_k^{\dagger}\mathbf{w}_k \tag{6}$$

$$\text{s.t. } (C1): \frac{|\mathbf{w}_k^{\dagger}\mathbf{h}_i|^2}{\sum_{\ell\neq k}|\mathbf{w}_{\ell}^{\dagger}\mathbf{h}_i|^2+\sigma_{R,i}^2+\sigma_{D,i}^2} \geq \gamma_i, \quad \forall \Xi[(i,k,\ell)|\psi], \tag{7}$$

$$(C2): \mathcal{E}_j^{\mathcal{N}} \geq \xi_j, \forall j \in \mathcal{Z}_{Z+1}, \tag{8}$$

where γ_i is the SINR threshold at the i^{th} user, and ξ_j is the demanded harvested energy at j^{th} user (where i can be equal to j for some cases, in general). It is noteworthy that the SINR constraint in (7) may be equivalently interchanged by a rate constraint, as proved in Appendix A. We define the following metric to assist $(C1)$, as a conditional indicator for the three scenarios

$$\Xi[(i,k,\ell)|\psi] = \begin{cases} \psi(a): \ \forall i \in \mathcal{Z}_k, \ \forall k \in \{1,\ldots,Z\}, \\ \qquad \forall \ell \in \{1,\ldots,Z+1\}, \\ \psi(b): \ \forall i \in \mathcal{Z}_k, \ \forall k \in \{1,\ldots,Z\}, \\ \qquad \forall \ell \in \{1,\ldots,Z\}, \\ \psi(c): \ \forall i,\forall k,\forall \ell \in \{1,\ldots,K\}, \end{cases} \tag{9}$$

where $\psi(a), \psi(b)$, and $\psi(c)$ represents the SMEP, JMEP and PIEP scenarios, respectively. The indicator metric $\Xi[(i,k,\ell)|\psi]$ implies that the selections of (i,k,ℓ) are conditional according to the chosen scenario, i.e., ψ, where ψ corresponds to $\psi(a)$, and/or $\psi(b)$ and/or $\psi(c)$.

It is clear that the formulated problem $(P1)$ is not convex due to constraints $(C1)$ and $(C2)$ where its feasibility is dependent on γ_i and ξ_i, respectively. Moreover, it is interesting to note the hidden linearity aspect within the non-linear EH expression in (5), which can be useful in converting the non-linear EH constraint to a linear form, without loss of generality. The corresponding transformation is provided in (31) of Appendix B. In order to carry out further analysis, we simplify problem $(P1)$ without loss of generality, as follows

$$(P2): \min_{r,\{\mathbf{w}_k\}_{k=1}^{\Psi}} \ r \tag{10}$$

$$\text{s.t. } (C1): \frac{|\mathbf{w}_k^{\dagger}\mathbf{h}_i|^2}{\sum_{\ell\neq k}|\mathbf{w}_{\ell}^{\dagger}\mathbf{h}_i|^2+\sigma_{R,i}^2+\sigma_{D,i}^2} \geq \gamma_i, \quad \forall \Xi[(i,k,\ell)|\psi], \tag{11}$$

$$(C2): \zeta_j\left(\sum_{k=1}^{\Psi}|\mathbf{w}_k^{\dagger}\mathbf{h}_i|^2+\sigma_{R,j}^2\right) \geq \xi_j', \quad \forall j \in \mathcal{Z}_{Z+1}, \tag{12}$$

$$(C3): \sum_{k=1}^{\Psi}\mathbf{w}_k^{\dagger}\mathbf{w}_k \leq r, \tag{13}$$

where $r \in \mathbb{R}^+$ is the introduced slack variable to provide more tractability to the problem, and ξ_j' is the modified harvested energy demand at j^{th} user, defined as $\xi_j' = \zeta_j\Big(\sigma_{R,j}^2 + \beta - \frac{1}{\alpha}\ln\left(\frac{(1-\phi)(\mathcal{E}'-\xi_j)}{(1-\phi)\mathcal{E}'+\phi\xi_j}\right)\Big)$. Note that (C2) is a linear constraint introduced to simplify the problem. Proof for the corresponding transformation is provided in Appendix B. The introduction of the slack-variable r, constraints the total transmit power. Subsequently, at the optimum $r^{\star}$, the overall transmit power is minimized. Similar to $(P1)$, the problem $(P2)$ is non-convex. However, its formulation is more suitable for the proposed optimization method [16]. Therefore, we further investigate the problem in the succeeding sections.

B. Semi-Definite Programming (SDP) with Relaxation and Gaussian Randomization

We define $\mathbf{H}_i = \mathbf{h}_i\mathbf{h}_i^{\dagger}$, $\mathbf{w} = [\mathbf{w}_1^{\mathrm{T}} \ \mathbf{w}_2^{\mathrm{T}} \ldots \mathbf{w}_{\Psi}^{\mathrm{T}}]^{\mathrm{T}}$ and $\mathbf{W}_k = \mathbf{w}_k\mathbf{w}_k^{\dagger}$, $\forall k = \{1,\ldots,\Psi\}$. Then, with the help of these notations, $(P2)$ can be molded into a semi-definite programming (SDP) problem, where the non-convexity of $(P2)$ lies in the necessity to constrain the variable $\mathbf{W}_k$ to have unit rank. By dropping the rank-1 constraint, we obtain the following relaxed problem

$$(P3): \min_{r,\{\mathbf{W}_k\}_{k=1}^{\Psi}} \ r \tag{14}$$

$$\text{s.t. } (C1): \mathrm{Tr}\{\mathbf{H}_i\mathbf{W}_k\} - \gamma_i\sum_{\ell\neq k}\mathrm{Tr}\{\mathbf{H}_i\mathbf{W}_{\ell}\} \geq \gamma_i(\sigma_{R,i}^2+\sigma_{D,i}^2), \quad \forall \Xi[(i,k,\ell)|\psi], \tag{15}$$

$$(C2): \sum_{k=1}^{\Psi}\mathrm{Tr}\{\mathbf{H}_j\mathbf{W}_k\} \geq \frac{\xi_j'}{\zeta_j} - \sigma_{R,j}^2, \quad \forall j \in \mathcal{Z}_{Z+1}, \tag{16}$$

$$(C3): \sum_{k=1}^{\Psi}\mathrm{Tr}\{\mathbf{W}_k\} \leq r, \tag{17}$$

$$(C4): \mathbf{W}_k \succcurlyeq 0. \tag{18}$$

The SDP problem in $(P3)$ is convex and can be solved via well-known convex optimization techniques [21]. For our numerical evaluations, we make use of the convex programming tool CVX [22]. Following the semi-definite relaxation (SDR) in $(P3)$, the derivation of optimal $\mathbf{w}_k^{\star}$ requires a rank-1

approximation over $\mathbf{W}_k^\star$. This approximation may be obtained by using the Eigen-value Decomposition (EVD) [23] of $\mathbf{W}_k^\star$ and selecting the eigen-vector, which pertains to the maximum eigen-value. In this context, it is explicit that if $\text{rank}(\mathbf{W}_k^\star) = 1$, $\forall k$, then the obtained solutions are indeed optimal. However, the analytical results indicate towards the presence of multi-rank solutions corresponding to the precoder serving the EH group of users via SMEP, while unit rank solutions are obtained for all the other cases and scenarios. In this regard, Gaussian randomization method[3] [9] is employed to the former (i.e., precoder metric corresponding to the EH group of users) due to its high accuracy in yielding a rank-1 approximation of $\{\mathbf{W}_{Z+1}\}$ (in case of SMEP). In this context, SDR method with randomization is proven to be an effective and low-complexity approximation technique [16]. In [24], the authors have proposed a more effective method wherein besides using Gaussian randomization method, the rank-one constraint can also be replaced by other equivalent constraints, and then solved by using SCA and penalty method. However, alternative ways may be explored to further improve the approximation of the solution. In the succeeding section, we present a novel technique to address the multi-rank issue and provide better solutions in comparison with the SDR technique.

C. Novel Feasible Point Pursuit Successive Convex Approximation Method for Energy Optimization (FPP-SCA-e)

In this section, we present an enhanced technique motivated by the feasible-point pursuit and successive convex approximation (FPP-SCA), which was proposed as an effective alternative to SDR in [15], [16]. In contrast to the traditional FPP-SCA method applied to such frameworks [16], the technique proposed in this paper, FPP-SCA-e, takes care of an additional constraint of harvested energy demand at the intended users. It is clear that the problem $(P2)$ can be categorized within the general class of quadratically constrained quadratic problems (QCQPs), and thus a modified technique in-line with FPP-SCA can be developed which also takes into account an additional harvested energy constraint. To proceed, we define $\mathbf{w}_{\text{tot}} = [\mathbf{w}_1^\dagger, \mathbf{w}_2^\dagger, \ldots, \mathbf{w}_\Psi^\dagger]^\dagger$ such that the i^{th} SINR constraint reads as

$$\mathbf{w}_{\text{tot}}^\dagger \mathbf{\Lambda}_i \mathbf{w}_{\text{tot}} \leq -\gamma_i(\sigma_{R,i}^2 + \sigma_{D,i}^2), \tag{19}$$

where $\mathbf{\Lambda}_i = \mathbf{\Lambda}_i^{(+)} + \mathbf{\Lambda}_i^{(-)}$ with $\mathbf{\Lambda}_i^{(+)} = \gamma_i(\mathrm{I}_\Psi - \text{diag}\{\mathbf{e}_k\}) \otimes \mathbf{h}_i\mathbf{h}_i^\dagger$, $\mathbf{\Lambda}_i^{(-)} = -\text{diag}\{\mathbf{e}_k\} \otimes \mathbf{h}_i\mathbf{h}_i^\dagger, \forall i \in \mathcal{Z}_k$, with $k \in \{1, \ldots, \Psi\}$. Let $\boldsymbol{\omega}$ denote any random point so that by the definition of a semi-definite matrix $\mathbf{\Lambda}_i^{(-)}$ we have $(\mathbf{w}_{\text{tot}} - \boldsymbol{\omega})^\dagger \mathbf{\Lambda}_i^{(-)} (\mathbf{w}_{\text{tot}} - \boldsymbol{\omega}) \leq 0$. With further simplification, we express the linear constraint of $\mathbf{w}_{\text{tot}}$ around $\boldsymbol{\omega}$ as follows

$$\mathbf{w}_{\text{tot}}^\dagger \mathbf{\Lambda}_i^{(-)} \mathbf{w}_{\text{tot}} \leq 2\text{Re}\{\boldsymbol{\omega}^\dagger \mathbf{\Lambda}_i^{(-)} \mathbf{w}_{\text{tot}}\} - \boldsymbol{\omega}^\dagger \mathbf{\Lambda}_i^{(-)} \boldsymbol{\omega}. \tag{20}$$

Subsequently, the SINR constraint in (20) is given by

$$\mathbf{w}_{\text{tot}}^\dagger \mathbf{\Lambda}_i^{(+)} \mathbf{w}_{\text{tot}} + 2\text{Re}\{\boldsymbol{\omega}^\dagger \mathbf{\Lambda}_i^{(-)} \mathbf{w}_{\text{tot}}\} - \boldsymbol{\omega}^\dagger \mathbf{\Lambda}_i^{(-)} \boldsymbol{\omega} \leq -\gamma_i(\sigma_{R,i}^2 + \sigma_{D,i}^2), \tag{21}$$

[3]Based on the statistics outlined by the relaxed solution, precoding vectors are generated with the help of Gaussian distribution. The solution nearest to the relaxed upper bound is chosen after creating several re-scaled instances.

wherein the unknown variables are quadratic over a semi-definite matrix. Following a similar trend, the harvested energy constraint at the ϵ^{th} user can thus be represented as

$$\zeta_\epsilon \Big[\boldsymbol{\omega}^{(j)H} \mathbf{\Lambda}_\epsilon^{(-)} \boldsymbol{\omega}^{(j)} - 2\text{Re}\{\boldsymbol{\omega}^{(j)H} \mathbf{\Lambda}_\epsilon^{(-)} \mathbf{w}_{\text{tot}}\} - \mathbf{w}_{\text{tot}}^\dagger \hat{\mathbf{\Lambda}}_\epsilon^{(+)} \mathbf{w}_{\text{tot}} + \sigma_{R,\epsilon}^2 \Big] \geq \xi_\epsilon', \tag{22}$$

where $\hat{\mathbf{\Lambda}}_\epsilon^{(+)} = (\mathrm{I}_\Psi - \text{diag}\{\mathbf{e}_k\}) \otimes \mathbf{h}_\epsilon\mathbf{h}_\epsilon^\dagger$, $\forall \epsilon \in \mathcal{Z}_{Z+1}$, with $k \in \{1, \ldots, \Psi\}$. By adding the slack penalties $\mathbf{v} \in \mathbb{R}^+_{(Z+2)}$, the QCQP problem in $(P2)$ can be approximated as follows

$$(P4): \min_{r, \mathbf{w}_{\text{tot}}, \mathbf{v}} \; r + \lambda ||\mathbf{v}|| \tag{23}$$

$$\text{s.t.} \;\; (C1): \mathbf{w}_{\text{tot}}^\dagger \mathbf{\Lambda}_i^{(+)} \mathbf{w}_{\text{tot}} + 2\text{Re}\{\boldsymbol{\omega}^{(j)\dagger} \mathbf{\Lambda}_i^{(-)} \mathbf{w}_{\text{tot}}\} - \boldsymbol{\omega}^{(j)\dagger} \mathbf{\Lambda}_i^{(-)} \boldsymbol{\omega}^{(j)} \leq -\gamma_i(\sigma_{R,i}^2 + \sigma_{D,i}^2) + \mathrm{v}_{\mathcal{I}},$$
$$\forall \Xi[(i,k,\ell)|\psi], \; \mathcal{I} \in \{1, \ldots, Z\}, \tag{24}$$

$$(C2): \zeta_\epsilon \Big[\boldsymbol{\omega}^{(j)\dagger} \mathbf{\Lambda}_\epsilon^{(-)} \boldsymbol{\omega}^{(j)} - 2\text{Re}\{\boldsymbol{\omega}^{(j)\dagger} \mathbf{\Lambda}_\epsilon^{(-)} \mathbf{w}_{\text{tot}}\} - \mathbf{w}_{\text{tot}}^\dagger \hat{\mathbf{\Lambda}}_\epsilon^{(+)} \mathbf{w}_{\text{tot}} + \sigma_{R,\epsilon}^2 \Big] \geq \xi_\epsilon' - \mathrm{v}_{Z+1},$$
$$\forall \epsilon \in \mathcal{Z}_{Z+1}, \tag{25}$$

$$(C3): \mathbf{w}_{\text{tot}}^\dagger \mathbf{w}_{\text{tot}} \leq r + \mathrm{v}_{Z+2}, \tag{26}$$

where $r \in \mathbb{R}^+$, $\lambda \in \mathbb{R}$ is a fixed input parameter, $\boldsymbol{\omega}^{(j)}$ is the j^{th} instance of the introduced auxiliary variable, and $||\cdot||$ can be any vector norm. Herein, $(P4)$ is a convex QCQP and can be solved via well-known convex optimization techniques [21]. Similar to FPP-SCA as in [15], $(P4)$ is solved with starting point selection as $\boldsymbol{\omega}^{(j+1)} = \mathbf{w}_{\text{tot}}^{(j)}$ in each instance of the FPP-SCA-e algorithm. This iterative process is repeated until guaranteed convergence [15], [16]. The convergence proof is straight-forward. It is also noteworthy that the huge mismatch between the numerical values of the SINR and EH demands are needed to be compensated using the adequate selection of λ. This selection becomes crucial in enforcing the slack variables toward zero, thereby pushing the iterates towards the feasible region of $(P2)$. Since the modification to the problem is treated in the same way, i.e., eigenvalue separation; there is no change in the behavior of FPP-SCA-e technique with respect to the original FPP-SCA. In terms of the computational complexity, the FPP-SCA method is expected to be more efficient in comparison to the SDR, at high parameter value selections. Specifically, FPP-SCA involves computation of $\mathcal{O}(M\Psi + (Z+2) + 1)$ variables in contrast to SDR with $\mathcal{O}(M^2\Psi)$ optimization variables. It is clear that the former involves significantly lower number of parameter computations than the latter, provided the parameter value selections are high enough for numerical analysis.

IV. Numerical Results

In this section, we present the performance benefits of the proposed FPP-SCA-e over SDR, both employed on the three considered scenarios, viz., SMEP, JMEP, and PIEP. All these models and techniques are implemented using MATLAB R2017a, with optimization performed via convex programming tool CVX [22], and the solutions obtained with the help of SEDUMI solver.

Technique →		JMEP			SMEP			PIEP		
Antennas ↓	(γ_i, ξ_i) ↓	SDP	FPP-SCA-e	FPP-SCA-e$^+$	SDP	FPP-SCA-e	FPP-SCA-e$^+$	SDP	FPP-SCA-e	FPP-SCA-e$^+$
$M = 20$	(0.1 dB, 1 μJ)	25.4	5.6	31.0	43.7	6.9	50.4	268.8	15.9	284.0
	(25 dB, 1 μJ)	31.5	6.0	37.0	55.5	6.9	62.4	354.0	17.0	366.5
	(0.1 dB, 5 μJ)	25.4	5.6	31.0	47.7	6.8	55.0	275.6	16.8	288.0
	(25 dB, 5 μJ)	29.8	6.1	35.3	55.4	6.9	62.1	373.7	16.3	389.0
	AVERAGE	**28.025**	**5.825**	**33.575**	**50.575**	**6.875**	**57.475**	**318.025**	**16.500**	**331.875**
$M = 10$	(0.1 dB, 1 μJ)	2.4	5.3	7.6	2.7	6.5	9.3	4.9	14.6	17.8
	(25 dB, 1 μJ)	2.6	5.4	7.8	3.6	6.6	10.2	6.6	14.8	18.4
	(0.1 dB, 5 μJ)	2.4	5.3	7.8	2.8	6.4	9.4	5.9	14.8	18.5
	(25 dB, 5 μJ)	2.9	5.7	8.2	3.5	6.5	10.0	7.6	14.9	20.4
	AVERAGE	**2.575**	**5.425**	**7.850**	**3.150**	**6.500**	**9.725**	**6.250**	**14.775**	**18.775**

TABLE I: Execution time-complexity analysis (in seconds) of the proposed methods.

Technique / ξ_i	SDP	FPP-SCA-e	FPP-SCA-e$^+$
1 μJ	10.6347 dBW	10.1224 dBW	9.4784 dBW
2 μJ	13.6151 dBW	12.8914 dBW	12.4496 dBW
3 μJ	15.3523 dBW	14.7874 dBW	14.0671 dBW
4 μJ	16.5805 dBW	15.7903 dBW	15.5425 dBW
5 μJ	17.5288 dBW	16.8827 dBW	16.4088 dBW

TABLE II: Total Transmit Power for SMEP, optimized using SDP, SCA, and FPP-SCA-e$^+$ schemes, with γ_i = 5 dB and M = 16.

Technique / ξ_i	SDP	FPP-SCA-e	FPP-SCA-e$^+$
1 μJ	10.6347 dBW	9.8102 dBW	9.2665 dBW
2 μJ	13.6152 dBW	12.6895 dBW	12.3341 dBW
3 μJ	15.3527 dBW	14.8355 dBW	14.0506 dBW
4 μJ	16.5805 dBW	15.7481 dBW	15.4584 dBW
5 μJ	17.5288 dBW	16.7515 dBW	16.3696 dBW

TABLE III: Total Transmit Power for JMEP, optimized using SDP, SCA, and FPP-SCA-e$^+$ schemes, with γ_i = 5 dB and M = 16.

A. Simulation Set-up

Herein, the path-loss exponent for generating the channel realizations is chosen according to the ITU-R indoor model (2-floor office scenario) [25] as follows

$$\text{PL (in dB)} = 20\log_{10}(F) + N\log_{10}(D) + P_f(n) - 28, \quad (27)$$

where F is the operational frequency (in MHz), N is the distance power loss coefficient, D is the separation distance (in metres) between the transmitter and end-user(s) (with D > 1m), $P_f(n)$ = 15 + 4 (n-1) : is the floor penetration loss factor (in dB), and n is the number of floors between the transmitter and the end-user(s) (with $n \geq 0$). Specifically, the chosen parametric values are : F = 2.4 GHz, D = 5m (unless specified otherwise), N = 30, and $P_f(2)$ = 19 dB. The transmitter is assumed to be equipped with M = 20 antennas (unless specified otherwise) while K = 10 users are distributed within $(Z+1)$ = 5 groups as follows: $\mathcal{Z}_1 = \{U_1, U_3, U_4\}$, $\mathcal{Z}_2 = \{U_2, U_5\}$, $\mathcal{Z}_3 = \{U_6, U_8\}$, $\mathcal{Z}_4 = \{U_7, U_9, U_{10}\}$, and $\mathcal{Z}_5 = \{U_1, U_5, U_8, U_{10}\}$, where $\mathcal{Z}_5$ is the EH group of users while the remaining ($\mathcal{Z}_1$,$\cdots$, $\mathcal{Z}_4$) MC groups are comprised of ID users. We set to $\sigma^2_{R,i}$ = -110 dBW, $\sigma^2_{D,i}$ = -80 dBW and ζ_i = 0.6. Furthermore, an average of 500 random channel realizations (with random placement of end-users in every realization) is presented for each experiment. The constants for EH circuit are chosen as $\mathcal{E}'$ = 2.8 mJ, α = 1500, and β = 0.0022 [20].

B. Analysis of the FPP-SCA-e Solutions

Firstly, we focus on two different possibilities related to the initial point selection for $\boldsymbol{\omega}$ in the proposed method corresponding to $(P4)$. Let the starting point of $\boldsymbol{\omega}$ be denoted by $\widehat{\mathbf{w}}_{\text{tot}}$. The first possibility considers any random selection of $\widehat{\mathbf{w}}_{\text{tot}}$, which we term as FPP-SCA-e. Whereas for the second possibility, we provide the solution obtained via SDR as the input to $\widehat{\mathbf{w}}_{\text{tot}}$, which we refer to as FPP-SCA-e$^+$.

Next, we consider the computational complexities of the proposed techniques, wherein we present their run-time analysis in Table I using the tic-toc function in MATLAB R2017a, with all the reported values in seconds. On one hand, we observe that the execution time of SDP is faster than FPP-SCA-e for lower number of transmit antennas, in all the three scenarios. While on the other hand, significant run-time increment is seen in the case of SDP over FPP-SCA-e, for high number of transmit antennas. The FPP-SCA-e$^+$ technique relies on the starting point of SDP and thus behaves according to the execution times of both SDP and FPP-SCA-e. Specifically, the increased run-time for SDP ranges approximately between 150% and 200% (depending on the type of scheme chosen), whereas the increment in case of FPP-SCA-e is around 5% to 15% (for the three scenarios). From the application perspective regarding the implementation of the proposed methods in an actual system, it is worth mentioning that the computations pertaining the proposed algorithms may be employed via forthcoming C-ran architectures. The method works on the principle of increased computational resources in the cloud (i.e., where the computation of these algorithms can take place) [26], and hence these values are tolerable in an actual system.

Finally, we compare the three methods, namely, SDP, FPP-SCA-e, and FPP-SCA-e$^+$ in Tables II and III, respectively for the SMEP and JMEP scenarios. We find that the solution via SDR is considered the best starting point for FPP-SCA-e, as also illustrated for similar method in [16]. Hence, we consider only SDP and FPP-SCA-e$^+$ methods for further analysis.

C. Experimental Findings

This sub-section presents the results obtained via numerical experiments. In comparison with [15] and [16], we consider a more practical channel model whereas the problem formulated

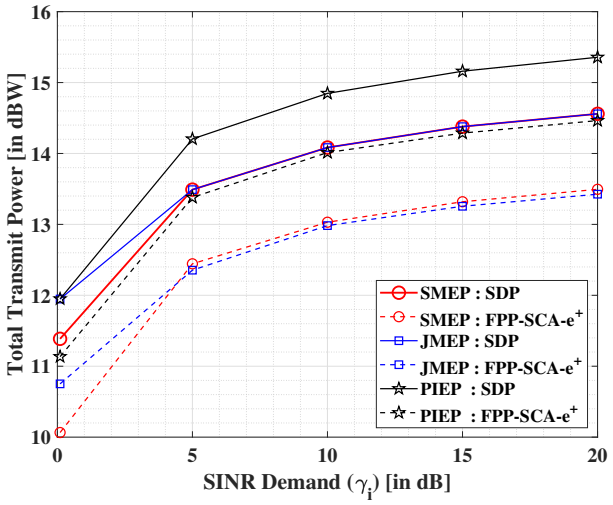

Fig. 5: Total transmit power versus the SINR demands at the users with SDP and FPP-SCA-e$^+$ techniques, where ξ_i = 2.5μJ.

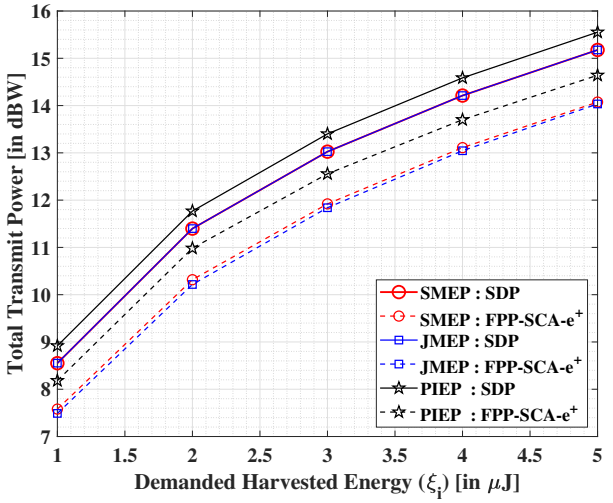

Fig. 6: Total transmit power versus the harvested energy demands at the users with SDP and FPP-SCA-e$^+$, where γ_i = 1 dB.

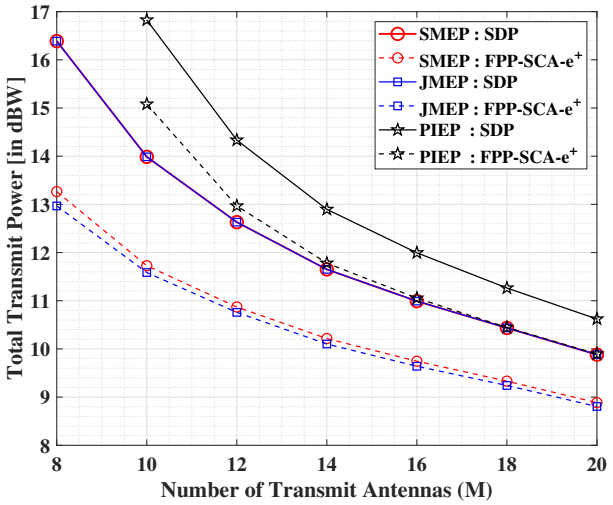

Fig. 7: Total transmit power versus number of antennas, using SDP and FPP-SCA-e$^+$ techniques, with γ_i = 5 dB and ξ_i = 1μJ.

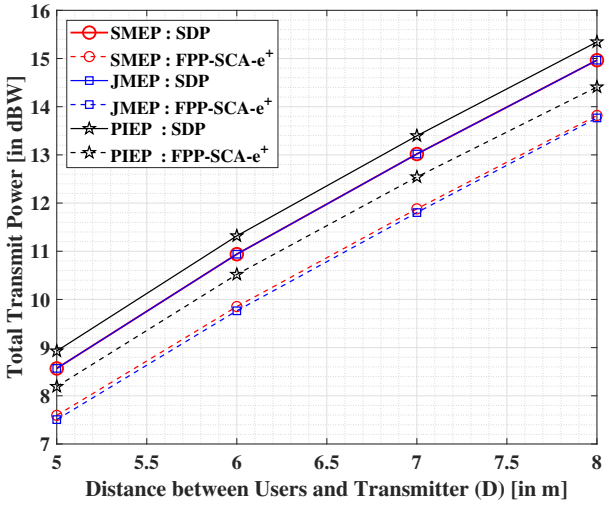

Fig. 8: Total transmit power versus the distance between the users and transmitter, with γ_i = 1 dB and ξ_i = 1μJ.

in this work involves an additional EH constraint. Based on the experimental findings, we set $\lambda = 10^{12}$ for FPP-SCA-e$^+$, and $\lambda = 10^{15}$ for FPP-SCA-e. These values are chosen to ensure the feasibility of considered problem in $(P4)$, and to force the slack variables in $\mathbf{v}$ towards zero. Specifically, with the considered channel model, and given that γ_i and ξ_i are both non-zeros, we propose to choose $\lambda \geq 1/(\min(\gamma_i/1\text{dB}, \xi_i/1\text{J}))$.

In Fig. 5, we investigate the performances of the three scenarios, namely, SMEP, JMEP, and PIEP, wherein the effect of increasing SINR demands on the total transmit power is examined for fixed ξ_i = 2.5 μJ. We observe that the total transmit power increases with growing SINR demands, for all the three above-mentioned scenarios. In addition, the proposed FPP-SCA-e$^+$ method provides a better estimate to the total transmit power in comparison to SDP. As noticed via both SDP and FPP-SCA-e$^+$ techniques, SMEP is found to perform better than JMEP in the low-SINR regimes while JMEP shows marginal advantages over SMEP in higher SINR regions. However, both JMEP and SMEP are seen to outperform PIEP in terms of total transmit power optimization for increasing SINR demands.

In Fig. 6, we present the impact on the total transmit power with increasing values of EH demands, where γ_i = 1 dB. The objective is seen to increase with growing EH demands for all the three considered scenarios, viz., SMEP, JMEP, and PIEP. The performances of SMEP and JMEP are found to be considerably better in comparison to PIEP, for both SDP and FPP-SCA-e$^+$ techniques. The optimized values of total transmit powers are nearly same for SMEP and JMEP in case of SDP. However, JMEP is observed to perform slightly better than SMEP in terms of transmit power optimization via FPP-SCA-e$^+$ method, for increasing EH demands.

Fig. 7, shows the result of increasing the number of transmit antennas on the total optimized transmit power for γ_i = 5 dB and ξ_i = 1 μJ. A general decreasing trend of total transmit power is observed from both SDP and FPP-SCA-

e$^+$ techniques for growing number of antennas, with latter (FPP-SCA-e$^+$) providing better solutions in comparison to the former (SDP). From an overall performance perspective, both JMEP and SMEP outperforms PIEP. However, similar outcomes are obtained for JMEP and SMEP through SDP, while JMEP is found to perform marginally better than SMEP. This marginal effect is due to the presence of an extra precoder in SMEP over JMEP.

We depict in Fig. 8 the performance analysis of the three scenarios (SMEP, JMEP and PIEP) in terms of total transmit power against increasing distance between the transmitter and users, with γ_i = 1 dB and ξ_i = 1 μJ. Please note that any point corresponding to (D) on the x-axis portrays the result for random arrangements of each user between (D) and $(D-1)$ for each instance of the experimental realizations. The total transmit power escalates significantly with increasing values of distances between the transmitter and users. Similar as above, we find that the SMEP and JMEP systems exceed over PIEP for both SDP and FPP-SCA-e$^+$ techniques. A slender gap is observed between the performances of SMEP and JMEP in case of FPP-SCA-e$^+$ technique while both shows identical performances with SDP.

D. Further investigation with variable users' categorization

Herein, we intend to further investigate the performances of the proposed SMEP, JMEP and PIEP schemes under the consideration of a variety of test-cases, with differing user categorizations within the MG and EH groups. For analytical convenience, we now fix a single group $\mathcal{G}_1$ for the ID users for MC operation and another group $\mathcal{G}_2$ comprising the EH users. In this context, let us first assume a scenario setting with incremental EH users, composed as follows: $\varsigma_1 := \{\mathcal{G}_1 = \{\mathcal{U}_1\}, \mathcal{G}_2 = \{\mathcal{U}_1\}\}$, $\varsigma_2 := \{\mathcal{G}_1 = \{\mathcal{U}_1\}, \mathcal{G}_2 = \{\mathcal{U}_1, \mathcal{U}_2\}\}$, $\varsigma_3 := \{\mathcal{G}_1 = \{\mathcal{U}_1\}, \mathcal{G}_2 = \{\mathcal{U}_1, \mathcal{U}_2, \mathcal{U}_3\}\}$, $\varsigma_4 := \{\mathcal{G}_1 = \{\mathcal{U}_1\}, \mathcal{G}_2 = \{\mathcal{U}_1, \mathcal{U}_2, \mathcal{U}_3, \mathcal{U}_4\}\}$, and $\varsigma_5 := \{\mathcal{G}_1 = \{\mathcal{U}_1\}, \mathcal{G}_2 = \{\mathcal{U}_1, \mathcal{U}_2, \mathcal{U}_3, \mathcal{U}_4, \mathcal{U}_5\}\}$. In this case, we choose an incremental trend of EH users, where one EH user is added to each incremental stage of ς_i, with $i = 1, \ldots, 5$. The MC group $\mathcal{G}_1$ is assumed to be fixed, having single ID user (i.e., $\mathcal{U}_1$) throughout. We show in Fig. 9 the results corresponding to the proposed SMEP, JMEP and PIEP schemes, with γ = 0.1 dB, ξ = 1 μJ, M = 16, and D = 5m. The bar plots in Fig. 9 follows an increasing trend for all the schemes with each increasing stage of scenario set-up. Intuitively, an increase in the number of EH users would require more power transmission from the transmit source. In this case, the performance of SMEP scheme is found to be superior to JMEP and PIEP schemes in terms of transmit power minimization. Therefore, in low SINR scenario, SMEP is the most preferred scheme.

The second analysis involves the selection of incremental sets of the ID users, comprised as follows : $\varpi_1 := \{\mathcal{G}_1 = \{\mathcal{U}_1\}, \mathcal{G}_2 = \{\mathcal{U}_1\}\}$, $\varpi_2 := \{\mathcal{G}_1 = \{\mathcal{U}_1, \mathcal{U}_2\}, \mathcal{G}_2 = \{\mathcal{U}_1\}\}$, $\varpi_3 := \{\mathcal{G}_1 = \{\mathcal{U}_1, \mathcal{U}_2, \mathcal{U}_3\}, \mathcal{G}_2 = \{\mathcal{U}_1\}\}$, $\varpi_4 := \{\mathcal{G}_1 = \{\mathcal{U}_1, \mathcal{U}_2, \mathcal{U}_3, \mathcal{U}_4\}, \mathcal{G}_2 = \{\mathcal{U}_1\}\}$, and $\varpi_5 := \{\mathcal{G}_1 = \{\mathcal{U}_1, \mathcal{U}_2, \mathcal{U}_3, \mathcal{U}_4, \mathcal{U}_5\}, \mathcal{G}_2 = \{\mathcal{U}_1\}\}$. As clearly indicated in the typesetting, we consider an incremental trend of ID users, where single ID user is added to each incremental setting of

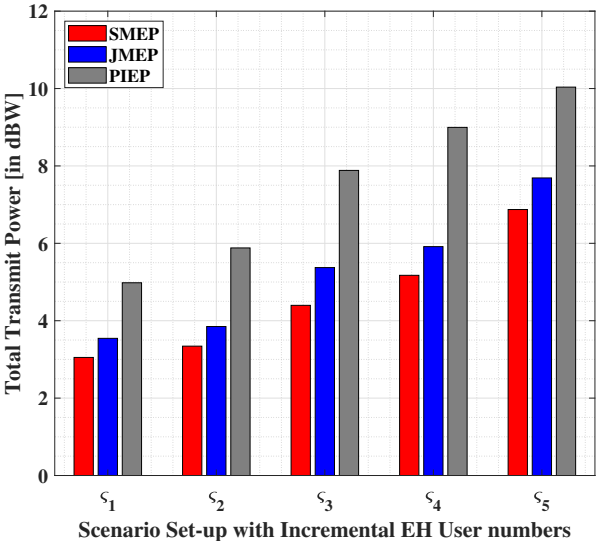

Fig. 9: The bar-plots to depict the outcomes of SMEP, JMEP and PIEP for the scenario setting with incremental EH users, where γ_i = 0.1 dB and ξ_i = 1μJ.

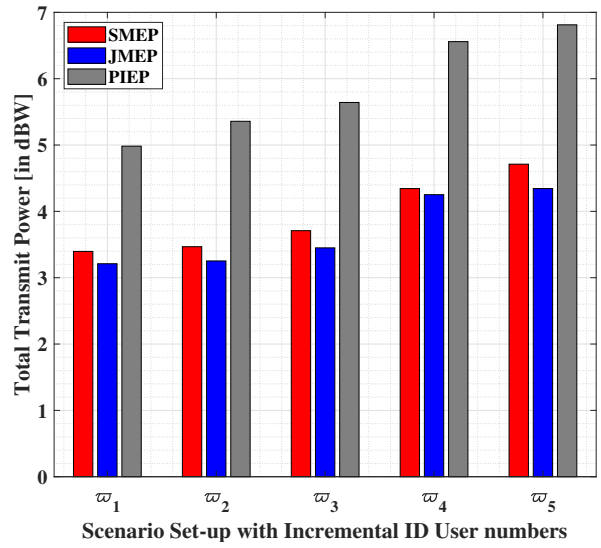

Fig. 10: The bar-plots to depict the outcomes of SMEP, JMEP and PIEP for the scenario setting with incremental ID users, where γ_i = 25 dB and ξ_i = 1μJ.

ϖ_i, with $i = 1, \ldots, 5$. We additionally assume the presence of single user ($\mathcal{U}_1$) in the EH group ($\mathcal{G}_2$) throughout, for this case. The performance measures of the proposed SMEP, JMEP and PIEP schemes are represented in Fig. 10 as bar-plots, where γ = 25 dB, ξ = 1 μJ, M = 16, and D = 5m. In Fig. 10, we plot the results corresponding to the total transmit power (in dBW) obtained via FPP-SCA-e$^+$ to compare the performances of SMEP, JMEP and PIEP schemes, with variation in the users' categorization as considered above. We observe that the the optimized transmit power for all the scenarios (i.e., SMEP, JMEP and PIEP) increases with increasing number of ID users in $\mathcal{G}_1$. This increase in the optimized transmit power is due to the corresponding additions of ID users, which implies that the high amount of power needs to be allocated in the precoders at

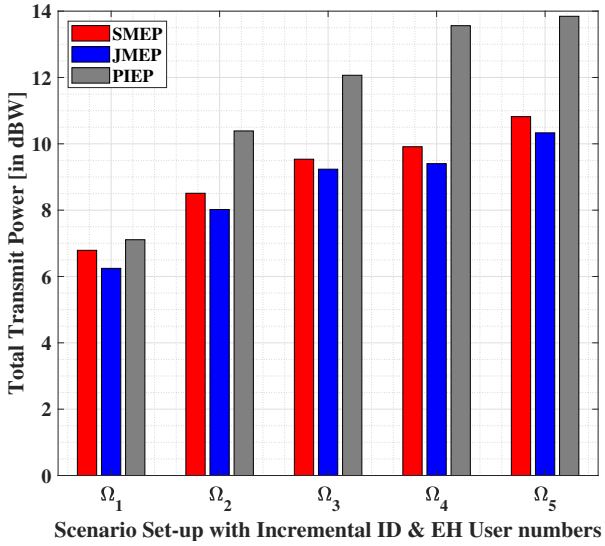

Fig. 11: The bar-plots to depict the outcomes of SMEP, JMEP and PIEP for the scenario setting with incremental ID and EH users, where γ_i = 5 dB and ξ_i = 1μJ.

the transmit source accordingly. However, the JMEP technique shows considerable advantages of SMEP and PIEP in terms of optimized transmit power. Thus, in the case of high-SINR regime, JMEP would be the best choice.

Finally, we assume the case with jointly incremental ID and EH users at each stage of the scenario set-up. We now assume two MC (i.e., $\mathcal{G}_1$ and $\mathcal{G}_2$) groups and one EH group ($\mathcal{G}_3$) to classify the users. The selection of users are comprised as follows: $\Omega_1 := \{\mathcal{G}_1 = \{\mathcal{U}_1\}, \mathcal{G}_2 = \{\mathcal{U}_6\}, \mathcal{G}_3 = \{\mathcal{U}_1, \mathcal{U}_6\}\}$, $\Omega_2 := \{\mathcal{G}_1 = \{\mathcal{U}_1, \mathcal{U}_2\}, \mathcal{G}_2 = \{\mathcal{U}_6, \mathcal{U}_7\}, \mathcal{G}_3 = \{\mathcal{U}_1, \mathcal{U}_2, \mathcal{U}_6, \mathcal{U}_7\}\}$, $\Omega_3 := \{\mathcal{G}_1 = \{\mathcal{U}_1, \mathcal{U}_2, \mathcal{U}_3\}, \mathcal{G}_2 = \{\mathcal{U}_6, \mathcal{U}_7, \mathcal{U}_8\}, \mathcal{G}_3 = \{\mathcal{U}_1, \mathcal{U}_2, \mathcal{U}_3, \mathcal{U}_6, \mathcal{U}_7, \mathcal{U}_8\}\}$, $\Omega_4 := \{\mathcal{G}_1 = \{\mathcal{U}_1, \mathcal{U}_2, \mathcal{U}_3, \mathcal{U}_4\}, \mathcal{G}_2 = \{\mathcal{U}_6, \mathcal{U}_7, \mathcal{U}_8, \mathcal{U}_9\}, \mathcal{G}_3 = \{\mathcal{U}_1, \mathcal{U}_2, \mathcal{U}_3, \mathcal{U}_4, \mathcal{U}_6, \mathcal{U}_7, \mathcal{U}_8, \mathcal{U}_9\}\}$, and $\Omega_5 := \{\mathcal{G}_1 = \{\mathcal{U}_1, \mathcal{U}_2, \mathcal{U}_3, \mathcal{U}_4, \mathcal{U}_5\}, \mathcal{G}_2 = \{\mathcal{U}_6, \mathcal{U}_7, \mathcal{U}_8, \mathcal{U}_9, \mathcal{U}_{10}\}, \mathcal{G}_3 = \{\mathcal{U}_1, \mathcal{U}_2, \mathcal{U}_3, \mathcal{U}_4, \mathcal{U}_5, \mathcal{U}_6, \mathcal{U}_7, \mathcal{U}_8, \mathcal{U}_9, \mathcal{U}_{10}\}\}$. Herein, we add a couple of ID and EH users each within the corresponding groups (i.e., one in each $\mathcal{G}_1$ and $\mathcal{G}_2$, and a couple in $\mathcal{G}_3$, respectively) at each growing stage of Ω_i, where $i = 1, \ldots, 5$. With these settings, we illustrate the performance measures of the proposed SMEP, JMEP and PIEP schemes in Fig. 11 by keeping γ = 5 dB, ξ = 1 μJ, M = 16, and D = 5m. In Fig. 11, we present the bar-plots corresponding to the optimized transmit power obtained with the help of the proposed FPP-SCA-e$^+$ technique. We observe an increasing trend at each incremental stage of the system setting with jointly increasing numbers of ID and EH users. The increase is due to the distribution of more power resources amongst the precoders for serving the correspondingly growing user numbers. Similar to the previous outcomes, we see the performance benefits of the JMEP scheme over the SMEP and PIEP schemes, concerning the optimization of the total transmit power. It is noteworthy that in this case, JMEP is the most preferred scheme.

E. Summary

The outcomes from the FPP-SCA-e$^+$ technique indicates towards the consideration of SMEP in low-SINR regime and JMEP otherwise. The overall outcomes via SDR technique imply that the solutions for JMEP and PIEP are (locally) optimal while (local) sub-optimal results are obtained for SMEP, which are rectified with the help of Gaussian randomization approach. From the hardware implementation perspective, this means that even with additional precoder(s) in comparison to JMEP, SMEP is seen to provide relatively better performance. However, both SMEP and JMEP provide comparably similar performances at higher demands of SINR implying that enough power could be harvested from the corresponding SINR beams and that the last group's energy precoder becomes redundant in case of SMEP[4]. It is important to highlight that the adoption of separate precoder designs for ID and EH operations does not only reduce the complexity at the transmit source, but also improves the overall system performance in terms of transmit power minimization. Besides, the proposed JMEP method may be considered a special case or a sub-system of SMEP, as inferred from the SDR solutions. Moreover, SMEP has another advantage where its flexibility may facilitate the adoption of different waveform designs, for the ID and EH operations, respectively. In this regard, recent studies, e.g., [19], have shown that the structure of the two waveforms can be rather different. The operation of PIEP involves same number of precoders as the users, which is good for individual users but it naturally imposes an overall high power consumption, thereby imposing large computational complexities. Moreover, PIEP would continue to demand more power allocation at the transmitter to provide the minimum (high) demands of SINR and EH demands at relevant users, and hence it cannot be considered as the best choice. Finally, it safe to say that SMEP may be chosen as the base system wherein a switch may be used to convert it to JMEP in the high SINR demand regime, while the demands of heterogeneous users are met via optimization of the corresponding precoder designs.

V. Conclusion

We proposed a novel technique named FPP-SCA-e, to address the problem of total transmit power minimization in three considered scenarios, namely, SMEP, JMEP, and PIEP. The developed technique was found to be suitable for solving a QCQP problem that consisted of both ID and EH users. Moreover, co-existence of heterogeneous user types was established under a practically motivated system model. Performance benefits of the FPP-SCA-e technique were shown over SDP via numerical results. From the systems perspective, SMEP was found to be most suitable candidate for practical implementation due to its flexible precoder designs and superior performance over JMEP and PIEP in the low-SINR regime. Moreover, this system may facilitate exclusive waveform designs targeting the ID and EH users separately, with an anticipated improvement in the overall system efficiency.

[4]It is worth mentioning that the case with contradictory constraints of low SINR and high EH demands is also difficult to realize in the JMEP scenario.

APPENDIX A
REPRESENTATION OF SINR CONSTRAINT AS A RATE CONSTRAINT FOR THE USERS

Herein, we re-express the SINR constraint in (7) as a rate constraint, to prove their equivalence in the presented context. From (7), we have

$$\frac{|\mathbf{w}_k^\dagger \mathbf{h}_i|^2}{\sum_{\ell\neq k}|\mathbf{w}_\ell^\dagger \mathbf{h}_i|^2+\sigma_{R,i}^2+\sigma_{D,i}^2} \geq \gamma_i, \forall \Xi[(i,k,\ell)|\psi]. \quad (28)$$

Assuming $\mathcal{B}$ as the bandwidth and given that both the sides in the constraint (28) are non-negative, we have the following

$$\mathcal{B}\log_2\left(1+\frac{|\mathbf{w}_k^\dagger \mathbf{h}_i|^2}{\sum_{\ell\neq k}|\mathbf{w}_\ell^\dagger \mathbf{h}_i|^2+\sigma_{R,i}^2+\sigma_{D,i}^2}\right) \geq \varrho_i, \quad (29)$$

where $\varrho_i = \mathcal{B}\log_2(1+\gamma_i), \forall \Xi[(i,k,\ell)|\psi]$. In this regard, γ_i can be up-scaled using $(2^{\frac{\varrho_i}{\mathcal{B}}}-1)$ according to the selection of ϱ_i, whereas ϱ_i may be down-scaled according to the selection of γ_i, to use any of the respective constraints in (28) and (29) equivalently.

APPENDIX B
CONVERSION OF NON-LINEAR ENERGY HARVESTING CONSTRAINT TO LINEAR CONSTRAINT

The non-linear EH constraint at i^{th} user is given by

$$\frac{\mathcal{E}'}{1-\phi}\cdot\left(\frac{1}{1+e^{(-\alpha(\sum_{k=1}^{\Psi}|\mathbf{w}_k^\dagger \mathbf{h}_i|^2)+\alpha\beta)}}-\phi\right) \geq \xi_i, \quad (30)$$

where ξ_i is the harvested energy demand at the i^{th} user within the feasibility set of problem constraints.

The expression in (30) can be re-arranged and written as

$$\frac{\mathcal{E}'}{1-\phi}\cdot\left(\frac{1}{1+e^{(-\alpha\mathcal{E}_i^{\mathcal{L}}/\zeta_i+\alpha\sigma_{R,i}^2+\alpha\beta)}}-\phi\right) \geq \xi_i. \quad (31)$$

Further simplification of (31) leads to the equivalent linear EH constraint

$$\mathcal{E}_i^{\mathcal{L}} \geq \xi_i', \quad (32)$$

where

$$\xi_i' = \zeta_i\left(\sigma_{R,i}^2+\beta-\frac{1}{\alpha}\ln\left(\frac{(1-\phi)(\mathcal{E}'-\xi_i)}{(1-\phi)\mathcal{E}'+\phi\xi_i}\right)\right). \quad (33)$$

From (33), it is clear that ξ_i' is a modified (higher) version of ξ_i and that the constraints in (8) and (32) are equivalent. QED.

ACKNOWLEDGMENT

The authors would like to thank Dr. Steven Kisseleff, Dr. Ashok Bandi, Dr. Thang X. Vu and for their help and efforts in the form of fruitful discussions, which were valuable for enhancement of some details in the manuscript.

REFERENCES

[1] S. Gautam, E. Lagunas, S. Kisseleff, S. Chatzinotas and B. Ottersten, "Successive Convex Approximation for Transmit Power Minimization in SWIPT-Multicast Systems," in *ICC 2020 - 2020 IEEE International Conference on Communications (ICC)*, 2020, pp. 1–7.

[2] Q. Shi, L. Liu, W. Xu, and R. Zhang, "Joint Transmit Beamforming and Receive Power Splitting for MISO SWIPT Systems," *IEEE Trans. Wireless Commun.*, vol. 13, no. 6, pp. 3269–3280, June 2014.

[3] S. Gautam, E. Lagunas, S. Chatzinotas, and B. Ottersten, "Wireless Multi-group Multicast Precoding with Selective RF Energy Harvesting," in *27th European Sig. Processing Conf. (EUSIPCO)*, September 2019.

[4] S. Gautam, E. Lagunas, A. Bandi, S. Chatzinotas, S. K. Sharma, T. X. Vu, S. Kisseleff and B. Ottersten, "Multigroup Multicast Precoding for Energy Optimization in SWIPT Systems With Heterogeneous Users," *IEEE Open Journal of the Communications Society*, vol. 1, pp. 92–108, 2020.

[5] R. Tandon, S. A. Jafar, S. Shamai, and H. V. Poor, "On the Synergistic Benefits of Alternating CSIT for the MISO Broadcast Channel," *IEEE Trans. Inf. Theory*, vol. 59, no. 7, pp. 4106–4128, July 2013.

[6] L. R. Varshney, "Transporting information and energy simultaneously," in *IEEE Int. Symp. Inf. Theory*, July 2008, pp. 1612–1616.

[7] M. R. A. Khandaker and K. Wong, "SWIPT in MISO Multicasting Systems," *IEEE Wireless Commun. Lett.*, vol. 3, no. 3, pp. 277–280, June 2014.

[8] Z. Ding, C. Zhong, D. W. K. Ng, M. Peng, H. A. Suraweera, R. Schober, and H. V. Poor, "Application of smart antenna technologies in simultaneous wireless information and power transfer," *IEEE Comm. Mag.*, vol. 53, no. 4, pp. 86–93, April 2015.

[9] N. D. Sidiropoulos, T. N. Davidson, and Z.-Q. Luo, "Transmit beamforming for physical-layer multicasting," *IEEE Trans. Signal Process.*, vol. 54, no. 6, pp. 2239–2251, June 2006.

[10] M. Alodeh, D. Spano, A. Kalantari, C. G. Tsinos, D. Christopoulos, S. Chatzinotas, and B. Ottersten, "Symbol-Level and Multicast Precoding for Multiuser Multiantenna Downlink: A State-of-the-Art, Classification, and Challenges," *IEEE Commun. Surveys Tuts.*, vol. 20, no. 3, pp. 1733–1757, thirdquarter 2018.

[11] E. Karipidis, N. D. Sidiropoulos and Z.-Q. Luo, "Convex Transmit Beamforming for Downlink Multicasting to Multiple Co-Channel Groups," in *Proc. IEEE Int. Conf. Acoust. Speech Signal Process.*, 2006, vol. 5, pp. V–V.

[12] D. Christopoulos, S. Chatzinotas and B. Ottersten, "Weighted Fair Multicast Multigroup Beamforming Under Per-antenna Power Constraints," *IEEE Trans. Signal Process.*, vol. 62, no. 19, pp. 5132–5142, 2014.

[13] Ö. T. Demir and T. E. Tuncer, "Multi-group multicast beamforming for simultaneous wireless information and power transfer," in *23rd European Sig. Processing Conf. (EUSIPCO)*, Aug 2015, pp. 1356–1360.

[14] Ö. T. Demir and T. E. Tuncer, "Antenna Selection and Hybrid Beamforming for Simultaneous Wireless Information and Power Transfer in Multi-Group Multicasting Systems," *IEEE Trans. Wireless Comm.*, vol. 15, no. 10, pp. 6948–6962, Oct 2016.

[15] O. Mehanna, K. Huang, B. Gopalakrishnan, A. Konar, and N. D. Sidiropoulos, "Feasible Point Pursuit and Successive Approximation of Non-Convex QCQPs," *IEEE Signal Process. Lett.*, vol. 22, no. 7, pp. 804–808, July 2015.

[16] D. Christopoulos, S. Chatzinotas, and B. Ottersten, "Multicast multigroup beamforming under per-antenna power constraints," in *IEEE Int. Conf. Comm. (ICC)*, June 2014, pp. 4704–4710.

[17] D. Christopoulos, S. Chatzinotas, and B. Ottersten, "Multicast Multigroup Precoding and User Scheduling for Frame-Based Satellite Communications," *IEEE Trans. Wireless Commun.*, vol. 14, no. 9, pp. 4695–4707, 2015.

[18] H. Zhou and M. Tao, "Joint multicast beamforming and user grouping in massive MIMO systems," in *2015 IEEE International Conference on Communications (ICC)*, 2015, pp. 1770–1775.

[19] B. Clerckx and E. Bayguzina, "Waveform Design for Wireless Power Transfer," *IEEE Trans. Signal Process.*, vol. 64, no. 23, pp. 6313–6328, 2016.

[20] J. Guo, H. Zhang, and X. Zhu, "Theoretical analysis of RF-DC conversion efficiency for class-F rectifiers," *IEEE Trans. Microw. Theory Techn.*, vol. 62, no. 4, pp. 977–985, 2014.

[21] S. Boyd and L. Vandenberghe, *Convex optimization*, Cambridge university press, 2004.

[22] M. Grant and S. Boyd, "CVX: Matlab software for disciplined convex programming, version 2.1," http://cvxr.com/cvx, Mar. 2014.

[23] K. Krishnan, *Linear programming (LP) approaches to semidefinite programming (SDP) problems*, Ph.D. thesis, Citeseer, 2002.

[24] X. Zhou, F. Shu S. Yan, an Q. Wu, and D. W. K. Ng, "Intelligent Reflecting Surface (IRS)-Aided Covert Wireless Communication with Delay Constraint," *arXiv e-prints*, Nov. 2020.

[25] P. Series, "Propagation data and prediction methods for the planning of indoor radiocommunication systems and radio local area networks in the frequency range 900 MHz to 100 GHz," *Recommendation ITU-R*, pp. 1238–7, 2012.

[26] R. G. Stephen and R. Zhang, "Fronthaul-Limited Uplink OFDMA in Ultra-Dense CRAN With Hybrid Decoding," *IEEE Trans. Veh. Technol.*, vol. 66, no. 10, pp. 9074–9084, 2017.

Sumit Gautam (S'14-M'20) received the B.Tech. degree (Hons.) in electronics and communication engineering from the LNM Institute of Information Technology (Deemed University), Jaipur, Rajasthan, India in 2013 and the MS degree in electronics and communication engineering by research from the International Institute of Information Technology (Deemed University), Hyderabad, Telangana, India in 2017 and the Ph.D. degree in computer science from the Interdisciplinary Centre for Security, Reliability, and Trust (SnT), University of Luxembourg, Luxembourg in 2020. He is currently working as a Research Associate/Post-Doctoral Researcher at the Interdisciplinary Centre for Security, Reliability, and Trust (SnT), University of Luxembourg, Luxembourg. His research interests include simultaneous wireless information and power transfer (SWIPT), caching, optimization methods, cooperative communications, backscatter communications, and precoding for multi-group multicast systems.

Eva Lagunas (S'09-M'13-SM'18) received the MSc and PhD degrees in telecom engineering from the Polytechnic University of Catalonia (UPC), Barcelona, Spain, in 2010 and 2014, respectively. She was Research Assistant within the Department of Signal Theory and Communications, UPC, from 2009 to 2013. During the summer of 2009 she was a guest research assistant within the Department of Information Engineering, Pisa, Italy. From November 2011 to May 2012 she held a visiting research appointment at the Center for Advanced Communications (CAC), Villanova University, PA, USA. She joined the Interdisciplinary Centre for Security, Reliability and Trust (SnT), University of Luxembourg, first as a Research Associate, and in 2018 as Research Scientist. Her research interests include radio resource management and general wireless networks optimization.

Symeon Chatzinotas (S'06-M'09-SM'13) received the M.Eng. degree in telecommunications from the Aristotle University of Thessaloniki, Thessaloniki, Greece, in 2003, and the M.Sc. and Ph.D. degrees in electronic engineering from the University of Surrey, Surrey, U.K., in 2006 and 2009, respectively. He is currently a Full Professor/Chief Scientist I and Co-Head of the SIGCOM Research Group with SnT, University of Luxembourg. He was a Visiting Professor with the University of Parma, Italy, and he was involved in numerous research and development projects for the National Center for Scientific Research Demokritos, the Center of Research and Technology Hellas, and the Center of Communication Systems Research, University of Surrey. He has coauthored more than 400 technical papers in refereed international journals, conferences, and scientific books. He was a co-recipient of the 2014 IEEE Distinguished Contributions to Satellite Communications Award, the CROWNCOM 2015 Best Paper Award, and the 2018 EURASIC JWCN Best Paper Award. He is currently the editorial board of the IEEE OPEN JOURNAL OF VEHICULAR TECHNOLOGY and the International Journal of Satellite Communications and Networking.

Björn Ottersten (S'87-M'89-SM'99-F'04) was born in Stockholm, Sweden, in 1961. He received the M.S. degree in electrical engineering and applied physics from Linköping University, Linköping, Sweden, in 1986, and the Ph.D. degree in electrical engineering from Stanford University, Stanford, CA, USA, in 1990. He has held research positions with the Department of Electrical Engineering, Linköping University, the Information Systems Laboratory, Stanford University, the Katholieke Universiteit Leuven, Leuven, Belgium, and the University of Luxembourg, Luxembourg. From 1996 to 1997, he was the Director of Research with ArrayComm, Inc., a start-up in San Jose, CA, USA, based on his patented technology. In 1991, he was appointed a Professor of signal processing with the Royal Institute of Technology (KTH), Stockholm, Sweden. From 1992 to 2004, he was the Head of the Department for Signals, Sensors, and Systems, KTH, and from 2004 to 2008, he was the Dean of the School of Electrical Engineering, KTH. He is currently the Director for the Interdisciplinary Centre for Security, Reliability and Trust, University of Luxembourg.

He was a recipient of the IEEE Signal Processing Society Technical Achievement Award in 2011 and the European Research Council advanced research grant twice, in 2009-2013 and in 2017-2022. He has co-authored journal papers that received the IEEE Signal Processing Society Best Paper Award in 1993, 2001, 2006, and 2013, and seven IEEE conference papers best paper awards. He has served as an Associate Editor for the IEEE TRANSACTIONS ON SIGNAL PROCESSING and the Editorial Board of the IEEE Signal Processing Magazine. He is currently a member of the editorial boards of EURASIP Signal Processing Journal, EURASIP Journal of Advances Signal Processing and Foundations and Trends of Signal Processing. He is a fellow of EURASIP.